

RESEARCH PAPER



Synthesis and evaluation of anticancer activities of 2- or 4-substituted 3-(*N*-benzyltriazolymethyl)-13 α -oestrone derivatives

Rebeka Jójárt^{a*}, Seyyed Ashkan Senobar Tahaei^{b*}, Péter Trungel-Nagy^a, Zoltán Kele^c, Renáta Minorics^b, Gábor Paragi^d, István Zupkó^b and Erzsébet Mernyák^a

^aDepartment of Organic Chemistry, University of Szeged, Szeged, Hungary; ^bDepartment of Pharmacodynamics and Biopharmacy, University of Szeged, Szeged, Hungary; ^cDepartment of Medicinal Chemistry, University of Szeged, Szeged, Hungary; ^dMTA-SZTE Biomimetic Systems Research Group, University of Szeged, Szeged, Hungary

ABSTRACT

2- or 4-Substituted 3-*N*-benzyltriazolymethyl-13 α -oestrone derivatives were synthesised via bromination of ring A and subsequent microwave-assisted, Pd-catalysed C(sp²)-P couplings. The antiproliferative activities of the newly synthesised brominated and phosphonated compounds against a panel of human cancer cell lines (A2780, MCF-7, MDA-MB 231) were investigated by means of MTT assays. The most potent compound, the 3-*N*-benzyltriazolymethyl-4-bromo-13 α -oestrone derivative exerted substantial selective cell growth-inhibitory activity against A2780 cell line with a submicromolar IC₅₀ value. Computational calculations reveal strong interactions of the 4-bromo derivative with both colchicine and taxoid binding sites of tubulin. Disturbance of tubulin function has been confirmed by photometric polymerisation assay.

ARTICLE HISTORY

Received 31 August 2020
Revised 28 September 2020
Accepted 13 October 2020

KEYWORDS

Hirao reaction; azide-alkyne cycloaddition; antiproliferative effect; tubulin polymerisation; molecular dynamics


1. Introduction

The development of anticancer agents is often based on synthetic modifications of endogenous compounds¹. However, this approach might be limited by the retained original biological activity of the biomolecule. This happens in the case of antiproliferative drug candidates based on sex hormones. Certain oestrone derivatives efficiently suppress the growth of different tumour cells, but their retained oestrogenic behaviour limits their application. Nevertheless, directed chemical modifications of the estrane core may lead to the reduction of oestrogenic action. The inversion of configuration at C-13 or opening of ring D results in core-modified oestrone derivatives with complete loss of oestrogenic activity^{2–5}. Accordingly, 13 α -oestrone and D-secoestrone are promising scaffolds for the development of antitumoral oestrone derivatives lacking hormonal side effects. Literature reveals certain potent anticancer oestrone derivatives, but their mechanism of action is often unclarified¹. There exist candidates acting via inhibition of oestrogen biosynthesis; however, the majority of this compound group target other objects, including transporter proteins or tubulin. Microtubules (MTs) consist of α - and β -tubulin heterodimers that play key role in cell division⁶. Drugs that interfere with tubulin polymerisation/depolymerisation dynamics might lead to suppression of the cell growth^{7–9}. Drugs that target the MT might be divided into two groups. MT destabilising agents (MDAs) prevent polymerisation of tubulin and promote depolymerisation, whereas MT stabilising agents (MSAs) promote polymerisation of tubulin and stabilise the polymer, preventing

depolymerisation. There exist six binding sites on tubulin polymer^{7,10,11}. MSAs, in general, bind reversibly to the taxoid binding site. Several antitubulin agents targeting vinca alkaloid or taxane sites (TBS) have been approved by Food and Drug Administration (FDA), but their application is limited due to their inefficiency against multidrug resistant (MDR) cells. On the other hand, colchicine site-binding candidates (CBS) are often still active against MDR cells, too. Combrestatin A-4 (CA-4) is a colchicine site-binding nanomolar antitubulin agent, arresting the cells in metaphase. Moreover, it is assigned as a potent vascular disrupting agent. It is of note that certain CA-4 derivatives are in clinical trials as chemotherapeutic agents. X-ray crystal structures of tubulin show that there are three zones and a bridge in this binding site. The typical colchicine site-binding agent consists of two aryl rings and a bridge, which determine the relative orientation of the rings¹¹. According to literature reports, replacement of methoxy groups with halogens and introduction of a triazole or tetrazole ring instead of an ethylene bridge might be a powerful strategy in the development of more effective antitubulin CA-4 derivatives (Figure 1)¹². The triazole heterocycle is widely used in drug development according to its favourable characteristics. It might enhance the stability against metabolic degradation and the H-bonding ability. Additionally, this heterocyclic ring is an excellent mimetic of a peptide bond¹³.

We have recently synthesised steroidal triazoles via the transformation of the phenolic OH group of the core-modified D-secoestrone scaffold¹⁴. 13 α and 13 β epimers of D-seco derivatives

CONTACT Gábor Paragi ✉ paragi@sol.cc.u-szeged.hu MTA-SZTE Biomimetic Systems Research Group, University of Szeged, Szeged, Hungary; István Zupkó ✉ zupko@pharm.u-szeged.hu Department of Pharmacodynamics and Biopharmacy, University of Szeged, Szeged, Hungary; Erzsébet Mernyák ✉ bobe@chem.u-szeged.hu Department of Organic Chemistry, University of Szeged, Dóm tér 8, Szeged H-6720, Hungary

 Supplemental data for this article can be accessed [here](#).

*These authors contributed equally to this work.

© 2020 The Author(s). Published by Informa UK Limited, trading as Taylor & Francis Group.

This is an Open Access article distributed under the terms of the Creative Commons Attribution License (<http://creativecommons.org/licenses/by/4.0/>), which permits unrestricted use, distribution, and reproduction in any medium, provided the original work is properly cited.

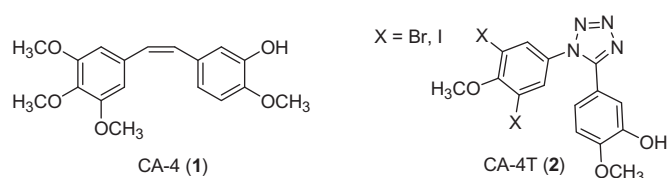


Figure 1. Structures of combrestatin A-4 and its tetrazolyl derivative.

were used as starting compounds. The triazole moiety was introduced onto C-3-O via CuAAC reaction of 3-(prop-2-ynyloxy) derivatives with benzyl azides. The evaluation of cell growth-inhibitory properties of 3-[[1-benzyl-1,2,3-triazol-4-yl]methoxy]-D-secooestrones against certain cervical, breast, and ovarian cancer cells was carried out. The determination of structure–activity relationship revealed that the antiproliferative effect greatly depends on both the orientation of the angular methyl group and the nature and size of the *para* substituent of the benzyl group. 13 β Derivatives seemed to be generally more active, but a 13 α compound displayed a substantial effect. The most potent compound displayed an IC₅₀ value in the low micromolar range. It was proved that the presence of the phenolic OH group is disadvantageous concerning the desired antiproliferative activity, but the introduction of a benzyl or, in particular, a 1-benzyl-1,2,3-triazol-4-yl moiety onto C-3-O leads to marked activity improvements. D-Secoestrone triazole **3** (Figure 2) was subjected to additional biological investigations in order to shed light on its mechanism of action¹⁵. The immunocytochemical flow cytometric analysis alluded to a cell cycle arrest at G2/M in HeLa cells with cell accumulation in the M phase. It was proved by an *in vitro* tubulin polymerisation assay that compound **3** significantly increases the maximum rate of microtubule formation. The antimigratory experiment showed that this triazole (**3**) inhibits the migration and invasion of HeLa cells. Based on these encouraging results, the 1-benzyl-1,2,3-triazol-4-yl moiety was introduced onto C-3-O of 13 α -oestrone bearing an intact ring D¹⁶. Our concept was to improve the one-micromolar IC₅₀ value of the best D-secoestrone triazole by synthesising new compounds bearing the same structural element at C-3-O, but on the other promising, hormonally inactive 13 α -oestrone scaffold. The most potent compound (**4a**) was that without any additional *para* substituent with IC₅₀ values in the submicromolar range. These results highlight the importance of 13 α -oestrone as a scaffold and the 3-*N*-benzyltriazolylmethyl moiety as a key element in the development of potent oestrone-based antiproliferative agents lacking oestrogenic action.

In recent years, we turned our attention on the synthesis of novel 2- or 4-substituted 13 α -oestrone derivatives. First ring A halogenations and then Pd-catalysed C–P cross-coupling reactions were carried out^{17,18}. Hirao reaction is widely used for the synthesis of arylphosphonates from aryl halides¹⁹. Variations of the reaction have been described under traditional thermal conditions or microwave-irradiation^{20–22}. Dialkyl phosphites are usually used as the reagents, Pd(PPh₃)₄ as the catalyst and Et₃N as the base. Our certain novel halo and phosphono 13 α -oestrone derivatives displayed outstanding inhibitory activities against enzymes (steroid sulfatase, STS and 17 β -hydroxysteroid dehydrogenase 1, 17 β -HSD1) involved in oestrogen biosynthesis. Concerning oestrogen-dependent diseases, the suppression of local oestrogen production might serve as an effective therapy. This strategy might be intensified by the inhibition of polypeptides transporting organic anions (OATPs), which are able to transport oestrone-3-sulfate (E1S) into cells^{23,24}. The desulphation of E1S and the stereospecific reduction of E1 result in E2 with a marked cell proliferative potential. Certain OATPs, known as E1S transporters, are overexpressed, among others, in breast and ovarian tumours. It is

of note that both 2-bromo- and 4-bromo-13 α -oestrone derivatives (**5** and **6**, Figure 3), synthesised recently, exerted outstanding 17 β -HSD1 inhibition (IC₅₀ = ~ 1 μ M). Compound **6**, however, displayed dual STS and 17 β -HSD1 inhibition. Additionally, 3-hydroxy-2-phosphonate **7** proved to be dual 17 β -HSD1 and OATP2B1 inhibitor with IC₅₀ values of 1–2 μ M, whereas its 3-benzyloxy counterpart (**8**) exhibited selective OATP2B1 inhibition with IC₅₀ = 0.2 μ M (Figure 3)¹⁸.

Based on our above-mentioned structure–activity results obtained in antiproliferative, tubulin polymerisation and OATP2B1 transport assays, our aim in the present study was to combine the key structural elements (highlighted in blue, green, and red in Figures 2 and 3) to get potent antiproliferative compounds. Here we disclose the synthesis of 3-*N*-benzyltriazolylmethyl-13 α -oestrone derivatives brominated or phosphonated at C-2 or C-4.

2. Results

2.1. Chemistry

The synthesis of 3-*N*-benzyltriazolylmethyl-13 α -oestrone derivatives substituted at C-2 or C-4 was started with the propargylation of 13 α -oestrone **9** (Scheme 1). The terminal alkyne function was introduced via our method established earlier¹⁶ using propargyl bromide as the reagent. The resulting 3-(prop-2-ynyloxy) compound (**10**) was subjected to CuAAC reaction with benzyl azides differing in their *para* substituent (R = H or *t*-Bu). The click reactions afforded the desired triazolyl derivatives (**4a** and **4b**) in high yields. The next transformation was the bromination of compounds **4a** and **4b**. Electrophilic substitutions were carried out with 1 equiv. of *N*-bromosuccinimide as a brominating agent. Halogenations occurred in *ortho* positions relative to the C-3-O function, yielding the two regioisomers in a ratio of **11**:**12** = 2:1. Bromo derivatives (**11a,b** or **12a,b**) were subjected to Pd-catalysed reactions with diethyl phosphite or diphenylphosphine oxide as coupling partners. Microwave-assisted Hirao couplings afforded new 2- or 4-phosphonated 3-*N*-benzyltriazolylmethyl-13 α -oestrone derivatives (**13–15**) in excellent yields. The structures of the newly synthesised bromides and phosphonates (**11–15**) were deduced from ¹H and ¹³C NMR spectra.

2.2. Antiproliferative activities

The new compounds (**11–15**) were evaluated for their cell growth-inhibitory action against an ovarian (A2780) and two breast (MCF-7 and MDA-MB-231) human adherent cancer cell lines. As a general tendency, ovarian cell line proved to be more sensitive for the tested agents than the utilised breast cancers. Certain newly synthesised derivatives exhibited substantial sub- or low-micromolar antiproliferative potentials (Table 1). Bromo derivatives (**11** and **12**) did not influence the growth of the tumour cells, except compound **12a**, which inhibited the proliferation of A2780 cells with a submicromolar IC₅₀ value. This test compound displayed substantially higher IC₅₀ values against the two other cell lines. Derivatives **13b** and **14a** proved to be the most potent in the phosphonate compound group with IC₅₀ values in the low micromolar range against all tested cell lines, which are comparable to those of reference agent cisplatin. Phosphonates exhibited a similar level of potency against MCF-7 and MDA-MB-231 cell lines. The only exception is compound **15b**, which did not exert considerable growth inhibitory action against MDA-MB-231 cells. The cancer selectivity of compound **12a** was tested by means of the MTT assay using the non-cancerous mouse embryo fibroblast cell line NIH/3T3. The treatment with compound **12a** resulted in a

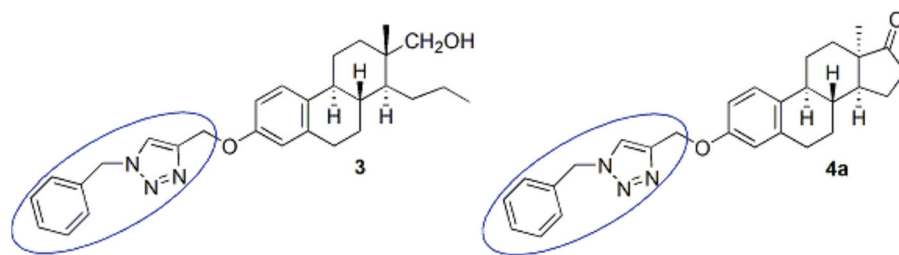


Figure 2. Structures of potent antiproliferative core-modified oestrone derivatives.

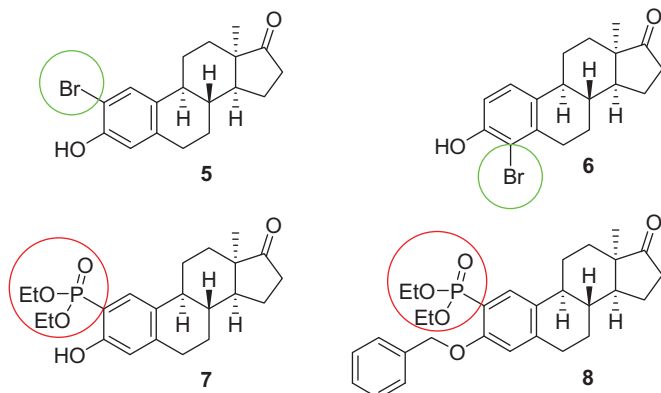


Figure 3. Structures of potent 17β-HSD1 and OATP2B1 inhibitors.

modest inhibition of cell growth ($28.73 \pm 1.26\%$ and $37.94 \pm 0.75\%$ in 10 and 30 μM , respectively) indicating the cancer selective property of the determined antiproliferative action.

2.3. Tubulin polymerisation assay

Previously, D-secoestrone triazole (**3**) was proved to significantly increase maximum rate of tubulin polymerisation¹⁵. Based on structural similarity between compound **3** and the newly synthesised **12a** owing the lowest IC_{50} value against ovarian cancer cell line A2780, **12a** was supposed to influence microtubule formation. To demonstrate our hypothesis, **12a** was subjected to a cell-free, *in vitro* tubulin polymerisation assay in two different concentrations (125 and 250 μM). The calculated maximum rate of tubulin polymerisation was increased by our test compound which was significant when **12a** was added in 250 μM concentration to the reaction mixture (Figure 4). Paclitaxel, the positive control agent recommended by the manufacturer, evoked a threefold increase in V_{max} (Figure 4).

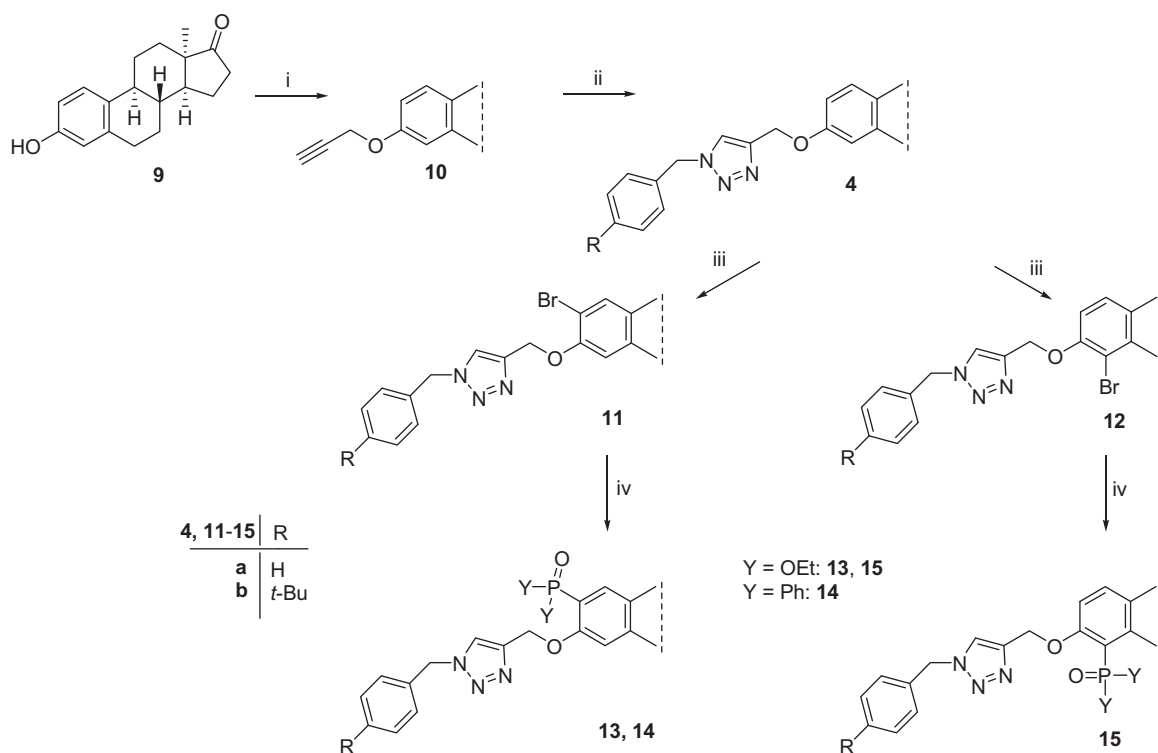
2.4. Computational simulations

First, docking studies have been performed for the newly synthesised most potent antiproliferative compound **12a** and for secosteroid **3** selected as a reference compound. Two potential binding sites, CBS and TBS, have been chosen on the tubulin polymer. MD investigations have been performed starting from the best docking poses of the compounds investigated. We found that the binding positions were stable for both compounds in both binding sites as they are presented by RMSD calculations for the ligands [see Figure S1(A–D) in Supplementary Materials]. Different MMGBSA binding energies collected in Table 2 clearly show that both compounds can bind to the regarded binding sites.

3. Discussion

3.1. Chemistry

The aim of the present work was to synthesise new 13 α -oestrone derivatives as potent antiproliferative agents against human cancer cell lines of reproductive origin. Our strategy included the combination of structural elements of our promising antiproliferative or enzyme inhibitor compounds synthesised recently. Ring A was chosen as the subject for transformations and positions C-2, C-3, and C-4 were aimed to modify. Concerning the feasibility of the planned transformations, the order of the reaction steps seemed to be crucial. The activating behaviour of the phenolic OH group enables fast and effective bromination of the aromatic ring; however, the regio- and chemoselectivity is very low. To enhance the selectivity, first the 3-OH group was etherified. We have recently published that bromination of 3-O-methyl-13 α -oestrone with 1 equiv. of NBS in dichloromethane results in a mixture of 2- and 4-bromo regioisomers in a ratio of 1:3¹⁷. Now we carried out the etherification of the phenolic OH group with a dual purpose: to get the two desired monobromo compounds regioselectively in the next step, and to introduce a terminal alkyne function onto C-3-O. We chose propargyl bromide as the reagent and performed the reaction under the conditions established earlier. The resulting phenolic ether (**10**) was suitable for the next bromination step, but the addition reactions on the terminal alkyne moiety had to be avoided. That is why we continued the sequence with the CuAAC reaction of the propargyl derivative (**10**) with two different benzyl azides ($R = \text{H}$ or *t*-Bu). Azide reagents were selected based on the cell growth-inhibitory results of 3-*N*-benzyltriazolylmethyl-13 α -oestrone derivatives synthesised and investigated earlier¹⁶. It has been established recently, that compound **4a** displayed outstanding antiproliferative action against certain cancer cell lines; however, its *para-t*-Bu counterpart **4b** did not influence cell growth markedly¹⁶. In this study, CuAAC reactions were performed using CuI as catalyst and PPh_3 as an accelerating phosphine ligand. The desired triazoles (**4a** and **4b**) were formed in excellent yields. The CuAAC reactions were followed by the bromination of the 3-*N*-benzyltriazolylmethyl compounds (**4a** and **4b**) with 1 equiv. of NBS in dichloromethane. Electrophilic brominations furnished the two *ortho* regioisomers in a ratio of **8:9** = 2:1 in high yields. Interestingly, regioselectivity of the bromination depends markedly on the nature and size of the C-3-O function. The difference in regioisomeric ratios compared to those of 3-O-Me derivatives might be explained by the steric hindrance of a more bulky 3-O substituent in 3-*N*-benzyltriazolylmethyl compounds **4a** and **4b**. In the last step, the 2- and 4-bromo regioisomers were subjected to Hirao couplings. In our earlier study, microwave-assisted conditions for the transformations of 2- and 4-bromo-3-O-methyl and -3-O-benzyl derivatives involved 10 mol% $\text{Pd}(\text{PPh}_3)_4$ as a catalyst, 1.3 equiv. of phosphite or phosphine oxide, and 3 equiv. K_2CO_3 in toluene¹⁸. The reaction time and temperature depended on the nature of the 3-O



Scheme 1. Synthesis of 2-substituted 3-*N*-benzyltriazolylmethyl-13 α -oestrone derivatives.

Table 1. Antiproliferative properties of the synthesised compounds

Comp.	Conc. (μM)	Inhibition (%) \pm SEM [calculated IC_{50}] ^a		
		A2780	MDA- MB-231	MCF-7
11a	10	44.87 \pm 0.09	47.49 \pm 1.21	29.06 \pm 1.42
	30	52.00 \pm 0.80 [21.51]	38.18 \pm 2.78	36.49 \pm 1.22
11b	10	30.18 \pm 2.35	24.39 \pm 2.20	– ^b
	30	33.94 \pm 2.70	23.92 \pm 1.07	–
12a	10	93.16 \pm 0.47	52.94 \pm 1.32	41.98 \pm 0.97
	30	95.43 \pm 0.42 [0.55]	53.81 \pm 2.43 [8.80]	52.50 \pm 0.94 [12.69]
12b	10	46.93 \pm 1.75	–	23.46 \pm 1.03
	30	54.72 \pm 0.70 [18.34]	–	29.19 \pm 2.94
13a	10	29.53 \pm 1.86	–	–
	30	90.85 \pm 0.40 [13.52]	35.95 \pm 3.17	43.54 \pm 2.63
13b	10	95.61 \pm 0.59	57.03 \pm 2.58	73.99 \pm 1.88
	30	99.73 \pm 0.21 [2.95]	98.93 \pm 0.20 [9.51]	95.52 \pm 0.23 [6.59]
14a	10	95.97 \pm 1.28	81.95 \pm 2.49	66.93 \pm 1.46
	30	98.06 \pm 0.89 [4.87]	98.52 \pm 0.10 [7.13]	92.52 \pm 1.08 [8.38]
14b	10	85.52 \pm 0.64	46.57 \pm 1.21	77.87 \pm 0.66
	30	95.82 \pm 0.12 [5.07]	71.28 \pm 1.23 [13.64]	90.69 \pm 0.18 [7.16]
15a	10	79.93 \pm 1.08	25.67 \pm 1.76	42.44 \pm 2.94
	30	99.50 \pm 0.03 [5.91]	96.87 \pm 0.28 [13.15]	91.04 \pm 1.49 [11.39]
15b	10	46.25 \pm 1.27	–	30.14 \pm 1.53
	30	92.05 \pm 0.86 [9.96]	34.79 \pm 2.20	77.45 \pm 1.56
Cisplatin		83.57 \pm 1.21	67.51 \pm 1.01	53.03 \pm 2.29
		95.02 \pm 0.28 [1.30]	87.75 \pm 1.10 [3.70]	86.90 \pm 1.24 [5.78]

^aMean value from two independent measurements with five parallel wells; standard deviation <20%.

^bInhibition values <20% are not presented.

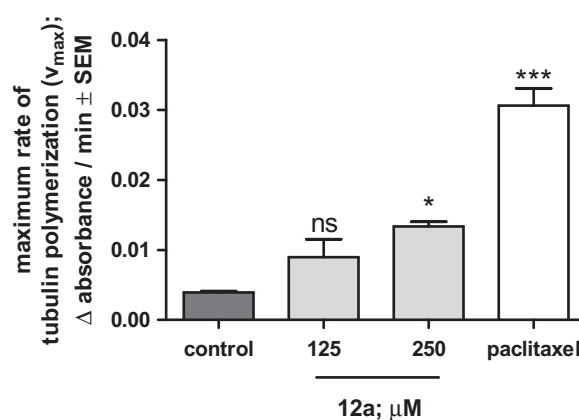


Figure 4. Effects of 12a and 10 μM paclitaxel on the calculated maximum reaction rate (V_{max}) of *in vitro* microtubule formation. Control: untreated samples. The experiment was performed in two parallels and the measurements were repeated twice. Each bar denotes the mean \pm SEM, $n=4$. ns, * and *** indicate $p > 0.05$, $p < 0.05$ and $p < 0.001$, respectively, compared with the control values.

Table 2. MMGBSA binding energies (in kcal/mol) of compound 3 and 12a in the CBS and TBS. Standard deviations of calculations are presented in parenthesis.

Compd.	CBS	TBS
3	–55.8 (8.3)	–58.8 (7.1)
12a	–63.3 (6.2)	–70.1 (6.5)

substituent. The transformations of 3-*O*-benzyl ethers required a more apolar solvent (toluene instead of acetonitrile) and harsher reaction conditions (150 $^{\circ}\text{C}$, 30 min). Based on these experiences, we performed the present couplings in toluene at 150 $^{\circ}\text{C}$, under microwave irradiation for 30 min. These conditions proved to be

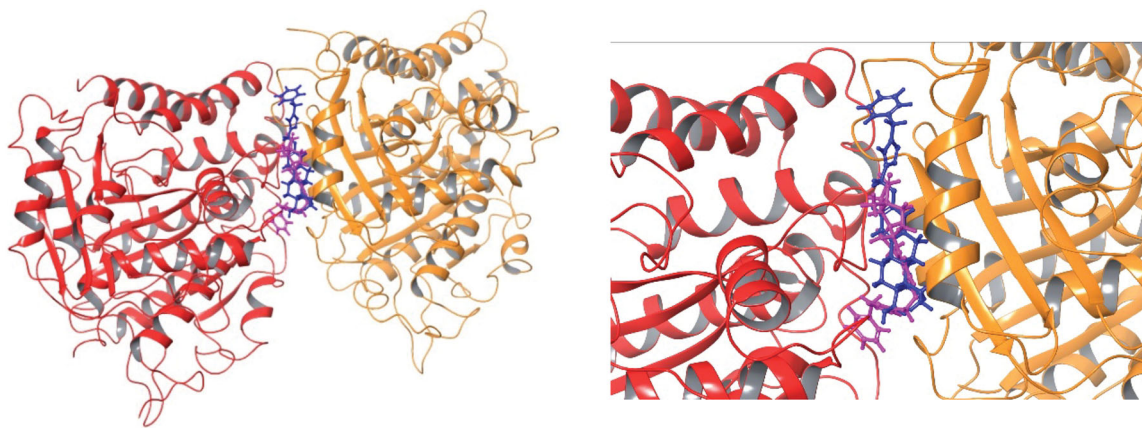


Figure 5. Best docking poses of compound **3** and **12a** in the CBS of tubulin dimer. The dark blue structure represents compound **3**, while purple marks compound **12a**.

excellent for the effective synthesis of the desired phosphonates (**13a,b**; **14a,b**, and **15a**), except for that of a 4-bromo derivative bearing a 4'-*t*-Bu substituent (**15b**). This coupling required longer irradiation (150 °C, 1 h), which might be attributed to steric factors.

3.2. Determination of the antiproliferative activities

We described earlier that triazole **4a** exerted outstanding inhibitory activities against A2780 and MCF-7 cell lines in the range of $IC_{50} = 0.5\text{--}0.6\ \mu\text{M}$. However, **4b**, its 4'-*t*-Bu counterpart did not have marked influence on the growth of the tested cell lines. Regarding the substantial difference in the antiproliferative potential of **4a** and **4b**, these two compounds have been selected for further transformations. Besides testing the newly synthesised compounds on A2780 (ovarian carcinoma) and MCF-7 (breast adenocarcinoma, expressing the oestrogen, progesterone, and androgen receptors), an additional cell line, the triple-negative breast carcinoma MDA-MB-231, was also included in our study. Based on the present results obtained for the phosphonates (Table 1), it can be stated, that this type of modification did not improve the high potency of parent compound **4a**. The cell growth-inhibitory potential of the phosphonates is far behind to that of unsubstituted **4a**. The low micromolar IC_{50} values of the phosphonates (**13b**, **14a,b**, and **15a**) reflect their moderate antiproliferative potential. Interestingly, phosphonates influenced the growth of A2780 cells most. Considering the two breast cancer cell lines with different receptorial status, no significant difference in growth-inhibitory activities have been observed. However, two compounds (**12a** and **14a**) proved to be more potent against the triple-negative MDA-MB-231 line. The presented pharmacological results are considered preliminary and, therefore, no conclusion can be made concerning the mechanism of the action. However, based on the comparison of the IC_{50} values obtained on the two breast cancer cell lines, a receptor-independent mechanism could be proposed. Results obtained for the 2-bromo compounds (**11a,b**) reveal that bromination at this position is disadvantageous concerning the antiproliferative potential against the tested cell lines. However, the other regioisomer without the 4'-*t*-Bu group (**12a**), proved to be highly potent with selective action against A2780 cells. The dependence of the cell growth-inhibitory potential on the regioisomerism is a very important structure–activity result.

Interestingly, the empirical rules established earlier proved to be valid for the bromo derivatives (**11a,b** and **12a,b**) as well. The presence of the 4'-*t*-Bu group on the newly introduced benzylic moiety was also detrimental.

The cancer selectivity of compound **12a** was tested by means of the MTT assay using the non-cancerous mouse embryo fibroblast cell line NIH/3T3. The growth inhibitory effect was found to be substantially lower than those against cancer cell lines. Since the inhibition of proliferation was less than 40% even at the highest concentration (30 μM), the IC_{50} value was not calculated but it is definitely above 30 μM . This kind of viability assay cannot be considered to be sufficient to declare a cancer-selective action. The huge difference in the determined antiproliferative properties may reflect a cell type-dependent action instead of a general toxic character indicating the relevance of the presented structure in lead-finding projects.

3.3. Tubulin polymerisation assay

Performing a 60-min-long tubulin polymerisation assay a direct effect of **12a** has been demonstrated on microtubule formation. The significant increase in V_{max} induced by our test compound is similar to the effects of other oestrone derivatives from D-secoalcohol²⁵ and D-secoestrone-triazole¹⁵ series. However, another ring A substituted cytotoxic oestradiol analogue, 2-methoxyestradiol, has been reported to inhibit tubulin polymerisation²⁶. This result is suitable for providing evidence about the final effect of our test compound on tubulin-microtubule system.

3.4. Computational simulations

We have demonstrated earlier that core-modified oestrone derivative **3** might be considered as an MSA. However, the majority of antitubulin oestrone derivatives described in literature belong to the MDA group, acting at the CBS of tubulin. From the comparison of the structures of the brominated combrestatine triazole **2** as an MDA and oestrone derivative **3**, it can be stated that they possess similar structural elements, such as the two aryl systems connected with a tetrazole or triazole bridge. It was shown by Beale et al. that the presence of bromines in compound **2** is advantageous concerning the antitubulin action. Interestingly, the two compounds belong to different MT targeting groups. Here we synthesised a new compound (**12a**) with structural similarity to both MT targeting agents **2** and **3**. Based on these structural

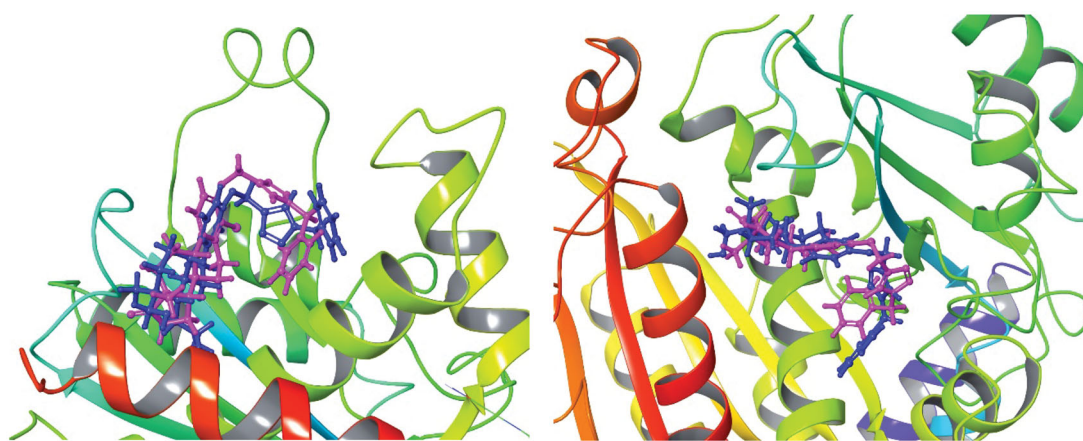


Figure 6. Best docking poses of compound **3** and **12a** in the TBS of tubulin monomer. The dark blue structure represents compound **3** while purple marks compound **12a**.

similarities and the substantial antiproliferative action of new derivative **12a**, here we performed computational studies to investigate the possible interaction of this compound with tubulin. Our selection, concerning the potential binding region of compound **12a** out of the known 6 possibilities^{7,10} taking tubulin surface, was based on the following considerations. (i) Oestrone derivatives usually interact with tubulin at the CBS¹¹. (ii) Ligands which promote polymerisation of tubulin usually bind to the TBS^{7,8}. Because we did not have experimental evidence for the exact binding position of compound **12a**, both potential binding sites (CBS and TBS) were considered. Secosteroid **3** was selected as a reference compound and, altogether, four different complexes were investigated in the simulations. Molecular docking studies were performed first in order to get the best poses for the following MD calculations. In Figures 5 and 6, we represented the binding poses of ligands **3** and **12a** in CBS and TBS, respectively. The purple structure always represents compound **12a**, while secoestrone **3** is represented in dark blue. It is clear, that in the TBS both compounds **3** and **12a** adopted almost the same binding position, while in the CBS the estrane cores occupied a common region, but in a reverse manner. Consequently, the 3-*N*-benzyltriazolylmethyl moiety oriented in an opposite way in the two cases.

Concerning binding preference order, SP docking score only helps to separate binding and non-binding molecules in a molecular pocket. However, it is not suitable to determine an accurate binding preference order; therefore, molecular dynamics (MD) calculations were performed. This allowed us to calculate binding energy at a more advanced level (MMGBSA method). Furthermore, calculations also provide information about the stability of the binding pose concerning the different ligand–protein complexes. It was established that the binding positions were stable in all four cases, even though the two compounds occupy the CBS in reversed manner (Table 2). Comparing binding energies at the same region, compound **12a** had always stronger interaction than compound **3**. Comparing binding energies at the different binding sites, compound **3** provided almost the same interaction energies in the two binding pockets, while compound **12a** had stronger interaction at the TBS. The strong interactions of compound **12a** indicate that the hormonally inactive 13 α -estrane core with certain ring A modifications might be a suitable scaffold in the design of potent MT targeting agents. Concerning its possible dual binding (at CBS and at TBS), it might be a promising candidate in the development of antitubulin drugs targeting MDR cells, too.

4. Materials and methods

4.1. Chemistry

Melting points (Mp) were determined with a Kofler hot-stage apparatus and are uncorrected. Elemental analyses were performed with a Perkin-Elmer CHN analyser model 2400 (PerkinElmer, Waltham, MA). Thin-layer chromatography: silica gel 60 F254; layer thickness 0.2 mm (Merck); eluents (ss): A: 50% ethyl acetate/50% hexane, B: ethyl acetate, C: 2% methanol/98% ethyl acetate, detection with I₂ or UV (365 nm) after spraying with 5% phosphomolybdic acid in 50% aqueous phosphoric acid and heating at 100–120 °C for 10 min. Flash chromatography: silica gel 60, 40–63 μ m (Merck, Kenilworth, NJ). Reactions under microwave irradiation were carried out with a CEM Corporation focussed microwave system, Model Discover SP. The maximum power of irradiation was 200 W. ¹H NMR spectra were recorded in DMSO-*d*₆, CDCl₃ solution with a Bruker DRX-500 instrument (Bruker, Billerica, MA) at 500 MHz, with Me₄Si as internal standard. ¹³C NMR spectra were recorded with the same instrument at 125 MHz under the same conditions. Mass spectrometry: full scan mass spectra of the compounds were acquired in the range of 50–1000 *m/z* with a Finnigan TSQ-7000 triple quadrupole mass spectrometer (Finnigan-MAT, San Jose, CA) equipped with a Finnigan electrospray ionisation source. Analyses were performed in positive ion mode using flow injection mass spectrometry with a mobile phase of 50% aqueous acetonitrile containing 0.1 v/v% formic acid. The flow rate was 0.3 ml/min. Five μ l aliquot of the samples were loaded into the flow. The ESI capillary was adjusted to 4.5 kV and N₂ was used as a nebuliser gas.

4.1.1. Synthesis of 3-(prop-2-ynyloxy)-13 α -estra-1,3,5(10)-triene (10)

3-Hydroxy-13 α -estra-1,3,5(10)-trien-17-one (**1**, 540 mg, 2.0 mmol) was dissolved in acetone (15 ml), then propargyl bromide [0.34 ml (80 wt.% in toluene), 3.0 mmol], and K₂CO₃ (1.94 g, 14 mmol) were added. The reaction mixture was stirred at 70 °C for 24 h, the solvent was then evaporated off, and the residue was purified by flash chromatography with EtOAc/CH₂Cl₂ = 2/98 as eluent. Compound **7** was obtained as a white solid (610 mg, 98%), mp 133–134 °C, R_f = 0.70 (ss B); Anal calcd. for C₂₁H₂₄O₂: C, 81.78; H, 7.84. Found: C, 81.93; H, 7.64. ¹H NMR: δ ppm H 1.06 (s, 3H, H-18); 2.49 (s, 1H, C \equiv CH); 2.83 (m, 2H, H-6); 4.65 (s, 2H, OCH₂); 6.68 (s, 1H, H-4); 6.77 (d, *J* = 8.5 Hz, 1H, H-2); 7.19 (d, *J* = 8.5 Hz, 1H, H-1). Compound **7** is identical with the compound described in Ref. [16].

4.1.2. Synthesis of 3-[[1-benzyl-1H-1,2,3-triazol-4-yl]methoxy]- and 3-[[1-(4-tert-butylbenzyl)-1H-1,2,3-triazol-4-yl]methoxy]-13 α -estra-1,3,5(10)-trien-17-one (4a and 4b)

To a stirred solution of 3-(prop-2-ynoxy)-13 α -estra-1,3,5(10)-trien-17-one **7** (616 mg, 2.0 mmol) in toluene (8 ml), Ph₃P (52 mg, 0.2 mmol), CuI (19.0 mg, 0.1 mmol), DIPEA (1.04 ml, 6.0 mmol), and benzylazide or 4-tert-butyl-benzylazide (1 equiv.¹⁶) were added. The reaction mixtures were refluxed for 2 h, cooled to rt and evaporated *in vacuo*. The residues were purified by flash chromatography with EtOAc/CH₂Cl₂ = 5/95 as eluent. Compound **4a** was obtained as a white solid (862 mg, 97%), mp 164–165 °C, R_f = 0.35 (ss C); ¹H NMR: δ ppm 1.05 (s, 3H, H-18); 2.80 (m, 2H, H-6); 5.14 (s, 2H, OCH₂); 5.51 (s, 2H, NCH₂); 6.67 (s, 1H, H-4); 6.75 (dd, *J* = 8.5 Hz, *J* = 2.0 Hz, 1H, H-2); 7.16 (d, *J* = 8.5 Hz, 1H, H-1); 7.27 (m, 2H, H-2', H-6'); 7.36 (m, 3H, H-3', H-4', H-5'); 7.50 (s, 1H, C = CH). Compound **4a** is identical with the compound described in Ref. [16].

Compound **4b** was obtained as a white solid (961 mg, 96%), mp 111–112 °C, R_f = 0.28 (ss C); ¹H NMR: δ ppm 1.05 (s, 3H, H-18); 1.31 (s, 3 \times 3H, C(CH₃)₃); 2.81 (m, 2H, H-6); 5.11 (s, 2H, OCH₂); 5.50 (s, 2H, NCH₂); 6.69 (s, 1H, H-4); 6.78 (m, 1H, H-2); 7.16–7.20 (overlapping multiplets, 3H, H-1, H-2', H-6'); 7.39 (d, 2H, H-3', H-5'); 7.55 (s, 1H, C = CH). Compound **4a** is identical with the compound described in Ref. [16].

4.1.3. General procedure for the bromination of triazoles 4a and 4b

Triazole **4a** or **4b** (442 mg or 498 mg, 1.00 mmol) was dissolved in dichloromethane (5 ml) and NBS (178 mg, 1.00 mmol) was added. The mixture was stirred at rt for 2.5 h, the solvent was then evaporated off and the crude product was purified by flash chromatography with EtOAc/hexane = 30/70 as eluent.

4.1.3.1. Synthesis of 3-[[1-benzyl-1H-1,2,3-triazol-4-yl]methoxy]-2-bromo-13 α -estra-1,3,5(10)-trien-17-one (11a) and 3-[[1-benzyl-1H-1,2,3-triazol-4-yl]methoxy]-4-bromo-13 α -estra-1,3,5(10)-trien-17-one (12a)

The first-eluting **12a** was obtained as a white solid (160 mg, 31%). Mp.: 188–190 °C. R_f = 0.66 (ss A). Anal calcd. for C₂₈H₃₀BrN₃O₂: C, 64.26; H, 5.81. Found: C, 64.34; H, 5.89. ¹H NMR (CDCl₃) δ ppm: 1.05 (s, 3H, H-18), 2.65 and 3.00 (2 \times m, 2 \times 1H, H-6), 5.24 (m, 2H, OCH₂), 5.52 (s, 2H, NCH₂), 6.87 (d, *J* = 8.6 Hz, 1H, H-2), 7.19 (d, *J* = 8.6, 1H, H-1), 7.27–7.28 (overlapping multiplets, 2H, H-2' and H-6'), 7.34–7.37 (overlapping multiplets, 3H, H-3', H-4' and H-6'), 7.58 (s, 1H, C = CH). ¹³C NMR (CDCl₃) δ ppm: 21.0 (CH₂), 25.0 (C-18), 28.3 (CH₂), 28.4 (CH₂), 31.6 (CH₂), 31.9 (CH₂), 33.4 (CH₂), 40.6 (CH), 41.7 (CH), 49.0 (CH), 50.0 (C-13), 54.2 (NCH₂), 63.7 (OCH₂), 111.4 (C-2), 115.2 (C-4), 122.7 (C = CH), 125.5 (C-1), 128.0 (2C, C-3' and C-5'), 128.8 (C-4'), 129.1 (2C, C-2' and C-6'), 134.5 (C-1'), 134.9 (C-10), 137.9 (C-5), 144.7 (C = CH), 152.6 (C-3), 221.4 (C-17). MS: [M + H]⁺ (79/81Br) 519 and 521.

The next-eluting **11a** was obtained as a white solid (319 mg, 61%). Mp.: 151–154 °C. R_f = 0.54 (ss A). Anal calcd. for C₂₈H₃₀BrN₃O₂: C, 64.26; H, 5.81. Found: 64.36; H, 5.88. ¹H NMR (CDCl₃) δ ppm: 1.05 (s, 3H, H-18), 2.70–2.82 (overlapping multiplets, 2H, H-6), 5.26 (m, 2H, OCH₂), 5.55 (s, 2H, NCH₂), 6.72 (s, 1H, H-4), 7.27–7.29 (overlapping multiplets, 2H, H-2', and H-6'), 7.38–7.39 (overlapping multiplets, 3H, H-3', H-4', H-6'), 7.66 (s, 1H, C = CH). ¹³C NMR (CDCl₃) δ ppm: 20.9 (CH₂), 25.0 (C-18), 28.0 (CH₂), 28.2 (CH₂), 30.0 (CH₂), 31.9 (CH₂), 33.4 (CH₂), 41.1 (CH), 41.3 (CH), 49.1 (CH), 50.1 (C-13), 54.8 (NCH₂), 63.1 (OCH₂), 109.4 (C-2), 114.3 (C-4), 123.2 (C = CH), 128.2 (2C, C-3', and C-5'), 129.1 (C-4'), 129.2 (2C, C-2', and C-6'), 130.8 (C-1), 133.8 (C-10), 134.7 (C-1'), 137.6 (C-5),

144.1 (C = CH), 152.1 (C-3), 221.4 (C-17). MS *m/z* (%): MS: [M + H]⁺ (79/81Br) 519 and 521.

4.1.3.2. Synthesis of 2-bromo-3-[[1-(4-tert-butylbenzyl)-1H-1,2,3-triazol-4-yl]methoxy]-13 α -estra-1,3,5(10)-trien-17-one (11b) and 4-bromo-3-[[1-(4-tert-butylbenzyl)-1H-1,2,3-triazol-4-yl]methoxy]-13 α -estra-1,3,5(10)-trien-17-one (12b)

The first-eluting **12b** was obtained as a white solid (98 mg, 17%). Mp.: 178–180 °C. R_f = 0.71 (ss A). Anal calcd. for C₃₂H₃₈BrN₃O₂: C, 66.66; H, 6.64. Found: 66.73; H, 6.72. ¹H NMR (CDCl₃) δ ppm: 1.05 (s, 3H, H-18), 1.31 (s, 9H, 4'-C(CH₃)₃), 2.65 and 3.00 (2 \times m, 2 \times 1H, H-6), 5.23 (m, 2H, OCH₂), 5.49 (s, 2H, NCH₂), 6.87 (d, *J* = 8.7 Hz, H-2), 7.18 (d, *J* = 8.7 Hz, 1H, H-1), 7.20 (d, *J* = 8.4 Hz, 2H, H-2', and H-6'), 7.38 (d, *J* = 8.4 Hz, 2H, H-3', and H-5'), 7.58 (s, 1H, C = CH). ¹³C NMR (CDCl₃) δ ppm: 21.0 (CH₂), 25.0 (C-18), 28.3 (CH₂), 28.4 (CH₂), 31.2 (3C, 4'-C(CH₃)₃), 31.6 (CH₂), 31.9 (CH₂), 33.4 (CH₂), 34.6 (4'-C(CH₃)₃), 40.6 (CH), 41.7 (CH), 49.0 (CH), 50.0 (C-13), 53.9 (NCH₂), 63.6 (OCH₂), 111.4 (C-2), 115.2 (C-4), 122.6 (C = CH), 125.5 (C-1), 126.0 (2C, C-3', and C-5'), 127.8 (2C, C-2', and C-6'), 131.5 (C-10), 134.9 (C-1'), 137.9 (C-5), 144.6 (C = CH), 151.9 and 152.6 (2C, C-3, and C-4'), 221.4 (C-17). MS: [M + H]⁺ (79/81Br) 575 and 577. Continued elution yielded first a mixture of **12b** (80 mg, 14%) and **11b** (140 mg, 24%), and then compound **11b** (218 mg, 38%) as a white solid. Mp.: 148–150 °C. R_f = 0.62 (ss A). Anal calcd. for C₃₂H₃₈BrN₃O₂: C, 66.66; H, 6.64. Found: 64.72; H, 6.72. ¹H NMR (CDCl₃) δ ppm: 1.05 (s, 3H, H-18), 1.37 (s, 9H, 4'-C(CH₃)₃), 2.70–2.82 (overlapping multiplets 2H, H-6), 5.22 (m, 2H, OCH₂), 5.49 (s, 2H, NCH₂), 6.74 (s, 1H, H-4), 7.20 (d, *J* = 8.4 Hz, 2H, H-2', and H-6'), 7.37–7.39 (overlapping multiplets, 3H, H-3', H-5', and H-1), 7.58 (s, 1H, C = CH). ¹³C NMR (CDCl₃) δ ppm: 20.9 (CH₂), 25.0 (C-18), 28.0 (CH₂), 28.2 (CH₂), 30.0 (CH₂), 31.2 (4'-C(CH₃)₃), 31.9 (CH₂), 33.4 (C), 34.6 (4'-C(CH₃)₃), 41.1 (CH), 41.3 (CH), 49.1 (CH), 50.0 (C-13), 53.9 (NCH₂), 63.7 (OCH₂), 109.5 (C-2), 114.3 (C-4), 122.6 (C = CH), 126.0 (2C, C-3', and C-5'), 127.8 (2C, C-2', and C-6'), 130.7 (C-1), 131.4 (C-10), 134.4 (C-1'), 137.4 (C-5), 144.6 (C = CH), 151.9 and 152.4 (2C, C-3, and C-4'), 221.3 (C-17). MS: [M + H]⁺ (79/81Br) 575 and 577.

4.1.4. General procedure for Hirao coupling of brominated triazoles (11a,b and 12a,b)

2- or 4-Bromo triazoles (**11a,b** or **12a,b**; 260 mg or 288 mg, 0.50 mmol), tetrakis(triphenylphosphine)palladium(0) (57.8 mg, 0.050 mmol, 10 mol%), potassium carbonate (104 mg, 0.75 mmol, 1.5 equiv.), diethyl phosphite (0.50 mmol, 69 mg) or diphenylphosphine oxide (0.50 mmol, 101 mg), and acetonitrile or toluene (5 ml) were added into a 10 ml Pyrex pressure vessel (CEM, Part #: 908035) with silicone cap (CEM, Part #: 909210). The mixture was irradiated in a CEM microwave reactor at 150 °C 30–60 min under stirring. The solvent was evaporated *in vacuo* and the residue was purified by flash chromatography.

4.1.4.1. Synthesis of (3-[[1-benzyl-1H-1,2,3-triazol-4-yl]methoxy]-13 α -estra-1,3,5(10)-trien-17-on-2-yl)-diethylphosphonate

The residue was purified by flash chromatography with MeOH/EtOAc = 2/98 as eluent. Compound **13a** was isolated as a white solid (84%). Mp.: 75–80 °C. R_f = 0.31 (ss B). Anal calcd. for C₃₂H₄₀N₃O₅P: C, 66.54; H, 6.98. Found: 66.62; H, 7.07. ¹H NMR (CDCl₃) δ ppm: 1.05 (s, 3H, H-18), 1.16 (t, *J* = 7.1 Hz, 6H, 2 \times OCH₂CH₃), 2.85 (m, 2H, H-6), 3.93–4.03 (overlapping multiplets, 4H, 2 \times OCH₂CH₃), 5.25 (m, 2H, OCH₂), 5.53 (s, 2H, NCH₂), 6.73 (d, *J* = 6.8 Hz, 1H, H-4), 7.27 (m, 2H, H-2', and H-6'), 7.39 (overlapping multiplets, 3H, H-3', H-4' and H-5'), 7.66 (d, *J* = 15.7 Hz, H-1), 7.83 (s, 1H, C = CH). ¹³C NMR

(CDCl₃) δ ppm: 16.3 (d, $J=6.3$ Hz, 2C: 2 \times OCH₂CH₃), 20.9 (CH₂), 25.0 (C-18), 27.8 (CH₂), 28.2 (CH₂), 30.6 (CH₂), 31.8 (CH₂), 33.3 (CH₂), 41.2 (CH), 41.3 (CH), 49.1 (CH), 50.1 (C-13), 54.3 (NCH₂), 61.9 (2C, 2 \times OCH₂CH₃), 63.1 (OCH₂), 112.8 (d, $J=9.9$ Hz, C-4), 114.1 (d, $J=188.9$ Hz, C-2), 123.1 (C=CH), 128.1 (2C, C-3', and C-5'), 128.7 (C-4'), 129.1 (2C, C-2', and C-6'), 132.6 (d, $J=13.8$ Hz, C-10), 132.8 (d, $J=8.1$ Hz, C-1), 134.5 (C-1'), 144.0 (2C, C-5, and C=CH), 157.4 (C-3), 221.4 (C-17). ³¹P NMR δ ppm: 17.8. MS m/z (%): 578 (100, [M + H]⁺).

4.1.4.2. Synthesis of (3-[[1-(4-tert-butylbenzyl)-1H-1,2,3-triazol-4-yl]methoxy]-13 α -estra-1,3,5(10)-trien-17-on-2-yl)-diethylphosphonate.

The residue was purified by flash chromatography with MeOH/EtOAc = 2/98 as eluent. Compound **13b** was isolated as a colourless oil (83%). $R_f=0.55$ (ss B). Anal calcd. for C₃₆H₄₈N₃O₅P: C, 68.23; H, 7.63. Found: 68.31; H, 7.72. ¹H NMR (CDCl₃) δ ppm: 1.05 (s, 3H, H-18), 1.15 (t, $J=7.1$ Hz, 6H, 2 \times OCH₂CH₃), 1.29 (s, 9H, 4'-C(CH₃)₃), 2.85 (m, 2H, H-6), 3.92–4.03 (overlapping multiplets, 4H, 2 \times OCH₂CH₃), 5.23 (m, 2H, OCH₂), 5.48 (s, 2H, NCH₂), 6.73 (d, $J=6.9$ Hz, 1H, H-4), 7.21 (d, $J=8.4$ Hz, 2H, H-2', and H-6'), 7.37 (d, $J=8.4$ Hz, 2H, H-3', and H-5'), 7.67 (d, $J=15.7$ Hz, 1H, H-1), 7.77 (s, 1H, C=CH). ¹³C NMR (CDCl₃) δ (ppm): 16.3 (d, $J=6.6$ Hz, 2C, 2 \times OCH₂CH₃), 20.9 (CH₂), 25.0 (C-18), 27.8 (CH₂), 28.2 (CH₂), 30.6 (CH₂), 31.2 (3C, 4'-C(CH₃)₃), 31.9 (CH₂), 33.3 (CH₂), 34.6 (4'-C(CH₃)₃), 41.2 (CH), 41.3 (CH), 49.1 (CH), 50.0 (C-13), 53.9 (NCH₂), 61.8 (2C, 2 \times OCH₂CH₃), 63.2 (OCH₂), 112.7 (d, $J=9.8$ Hz, C-4), 114.1 (d, $J=189.4$ Hz, C-2), 122.8 (C=CH), 125.9 (2C, C-3', and C-5'), 127.8 (2C, C-2', and C-6'), 131.6 (C-1'), 132.6 (d, $J=14.1$ Hz, C-10), 132.9 (d, $J=7.9$ Hz, C-1), 143.9 and 144.9 (2C, C-5, and C=CH), 151.8 (C-4'), 157.5 (C-3), 221.3 (C-17). ³¹P NMR δ ppm 17.8. MS m/z (%): 634 (100, [M + H]⁺).

4.1.4.3. Synthesis of (3-[[1-benzyl-1H-1,2,3-triazol-4-yl]methoxy]-13 α -estra-1,3,5(10)-trien-17-on-2-yl)diphenylphosphine oxide.

The residue was purified by flash chromatography with MeOH/EtOAc = 2/98 as eluent. Compound **14a** was isolated as a white solid (79%). Mp.: 117–120 °C. $R_f=0.28$ (ss C). Anal calcd. for C₄₀H₄₀N₃O₃P: C, 74.86; H, 6.28. Found: 74.93; H, 6.33. ¹H NMR (CDCl₃) δ ppm: 1.03 (s, 3H, H-18), 2.87 (m, 2H, H-6), 5.00 (m, 2H, OCH₂), 5.38 (s, 2H, NCH₂), 6.72–6.73 (overlapping multiplets, 2H), 7.15–7.17 (overlapping multiplets, 2H), 7.24–7.30 (m, 2H), 7.34–7.41 (overlapping multiplets, 6H), 7.55–7.63 (overlapping multiplets, 6H). ¹³C NMR (CDCl₃) δ ppm: 20.9 (CH₂), 25.0 (C-18), 27.9 (CH₂), 28.1 (CH₂), 30.7 (CH₂), 31.8 (CH₂), 33.4 (CH₂), 41.3 (CH), 41.5 (CH), 49.2 (CH), 50.1 (C-13), 54.0 (NCH₂), 62.5 (OCH₂), 112.4 (d, $J=6.9$ Hz, C-4), 117.6 (d, $J=105.5$ Hz, C-2), 122.6 (C=CH), 127.9 (2C, C-3', and C-5'), 128.0–128.2 (overlapping multiplets, 4C), 128.7 (C-4'), 129.1 (2C, C-2', and C-6'), 131.3 (m, 2C, C-4'' , and C-4'''), 131.6–131.8 (overlapping multiplets, 4C), 132.6 (C), 132.9 (d, $J=7.5$ Hz, C-1), 133.0 (C), 133.5 (C), 134.7 (C), 143.9 (C), 144.1 (C), 157.1 (C-3), 221.2 (C-17). ³¹P NMR δ ppm: 27.2. MS m/z (%): 642 (100, [M + H]⁺).

4.1.4.4. Synthesis of (3-[[1-(4-tert-butylbenzyl)-1H-1,2,3-triazol-4-yl]methoxy]-13 α -estra-1,3,5(10)-trien-17-on-2-yl)diphenylphosphine oxide.

The residue was purified by flash chromatography with MeOH/EtOAc = 2/98 as an eluent. Compound **14b** was isolated as a white solid (73%). Mp.: 205–208 °C. $R_f=0.42$ (ss C). Anal calcd. for C₄₄H₄₈N₃O₃P: C, 75.73; H, 6.93. Found: 75.79; H, 6.99. ¹H NMR (CDCl₃) δ ppm: 1.03 (s, 3H, H-18), 1.31 (s, 9H, 4'-C(CH₃)₃), 2.87 (m, 2H, H-6), 5.00 (d, $J=4.0$ Hz, 2H, OCH₂), 5.38 (s, 2H, NCH₂), 6.61 (s, 1H, C=CH), 6.71 (d, $J=5.5$ Hz, 1H, H-4), 7.09 (d, 2H), 7.21 (m,

2H), 7.27 (m, 2H), 7.33–7.40 (overlapping multiplets, 4H), 7.54–7.62 (overlapping multiplets, 4H), 7.64 (d, $J=14.2$ Hz, 1H, H-1). ¹³C NMR (CDCl₃) δ ppm: 20.9 (CH₂), 25.0 (C-18), 27.9 (CH₂), 28.1 (CH₂), 30.7 (CH₂), 31.2 (3C, 4'-C(CH₃)₃), 31.8 (CH₂), 33.4 (CH₂), 34.6 (4'-C(CH₃)₃), 41.3 (CH), 41.4 (CH), 49.1 (CH), 50.1 (C-13), 53.7 (NCH₂), 62.3 (OCH₂), 112.2 (d, $J=7.1$ Hz, C-4), 117.5 (d, $J=105.6$ Hz, C-2), 122.4 (C=CH), 125.9 (2C, C-3', and C-5'), 127.7 (2C, C-2', and C-6'), 127.9–128.1 (overlapping multiplets, 4C), 131.2 and 131.3 (C-4'' and C-4'''), 131.6–131.8 (overlapping multiplets, 4C), 131.6–134.0 (overlapping multiplets, 4C), 132.9 (d, $J=7.6$ Hz, C-1), 143.9 and 144.0 (C-5 and C=CH), 151.9 (C-4'), 156.9 (d, $J=3.0$ Hz, C-3), 221.4 (C-17). ³¹P NMR δ ppm: 26.9. MS m/z (%): 698 (100, [M + H]⁺).

4.1.4.5. Synthesis of (3-[[1-benzyl-1H-1,2,3-triazol-4-yl]methoxy]-13 α -estra-1,3,5(10)-trien-17-on-4-yl)-diethylphosphonate.

The residue was purified by flash chromatography with MeOH/EtOAc = 2/98 as an eluent. Compound **15a** was isolated as a white solid (72%). Mp.: 43–45 °C. $R_f=0.45$ (ss B). Anal calcd. for C₃₂H₄₀N₃O₅P: C, 66.54; H, 6.98. Found: C, 66.62; H, 7.07. ¹H NMR (CDCl₃) δ (ppm): 1.05 (s, 3H, H-18), 1.13 (t, $J=7.2$ Hz, 6H, 2 \times OCH₂CH₃), 3.26 (m, 2H, H-6), 3.88–4.01 (overlapping multiplets, 4H, 2 \times OCH₂CH₃), 5.21 (d, $J=3.8$ Hz, 2H, OCH₂), 5.53 (s, 2H, NCH₂), 6.87 (dd, $J=6.7$ Hz, $J=8.4$ Hz, 1H, H-2), 7.26–7.28 (m, 2H, H-2', and H-6'), 7.33–7.38 (overlapping multiplets, 2H, H-3', H-4', H-5', and H-1), 7.72 (s, 1H, C=CH). ¹³C NMR (CDCl₃) δ (ppm): 16.2 (2C, 2 \times OCH₂CH₃), 20.9 (CH₂), 24.9 (C-18), 28.2 (CH₂), 28.6 (CH₂), 29.3 (CH₂), 32.0 (CH₂), 33.3 (CH₂), 40.3 (CH), 41.7 (CH), 49.5 (CH), 50.1 (C-13), 54.2 (NCH₂), 61.3 (d, $J=5.2$ Hz, OCH₂CH₃), 61.4 (d, $J=5.2$ Hz, OCH₂CH₃), 63.7 (OCH₂), 110.9 (d, $J=10.1$ Hz, C-2), 115.1 (d, $J=182.0$ Hz, C-4), 122.8 (C=CH), 128.1 (2C, C-3', and C-5'), 128.7 (C-4'), 129.1 (2C, C-2', and C-6'), 131.5 (C-1), 134.4 (d, $J=14.0$ Hz, C-10), 134.6 (C-1'), 144.8 (d, $J=10.0$ Hz, C-5), 144.8 (C=CH), 145.0 (C), 159.0 (C-3), 221.6 (C-17). ³¹P NMR δ (ppm): 18.2. MS m/z (%): 578 (100, [M + H]⁺).

4.1.4.6. Synthesis of (3-[[1-(4-tert-butylbenzyl)-1H-1,2,3-triazol-4-yl]methoxy]-13 α -estra-1,3,5(10)-trien-17-on-4-yl)-diethylphosphonate.

The residue was purified by flash chromatography with EtOAc as an eluent. Compound **15b** was obtained as a white solid (70%). Mp.: 54–59 °C. $R_f=0.51$ (ss B). Anal calcd. for C₃₆H₄₈N₃O₅P: C, 68.26; H, 7.63. Found: C, 68.34; H, 7.69. ¹H NMR (CDCl₃) δ (ppm) 1.05 (s, 3H, H-18), 1.11 (t, $J=7.1$ Hz, 6H, 2 \times OCH₂CH₃), 1.29 (s, 9H, 4'-C(CH₃)₃), 3.25 (m, 2H, H-6), 3.88–4.01 (overlapping multiplets, 4H, 2 \times OCH₂CH₃), 5.20 (d, $J=3.9$ Hz, 2H, OCH₂), 5.49 (s, 2H, NCH₂), 6.87 (dd, $J=6.6$ Hz, $J=8.6$ Hz, 1H, H-2), 7.21 (d, $J=8.2$ Hz, 2H, H-3', and H-5'), 7.37 (overlapping multiplets, 3H, H-2', H-6', and H-1), 7.71 (s, 1H, C=CH). ¹³C NMR (CDCl₃) δ (ppm): 16.2 (d, $J=6.6$ Hz, 2C, 2 \times OCH₂CH₃), 20.9 (CH₂), 24.9 (C-18), 28.1 (CH₂), 28.6 (CH₂), 29.3 (CH₂), 31.2 (3C, 4'-C(CH₃)₃), 31.9 (CH₂), 33.3 (CH₂), 34.6 (4'-C(CH₃)₃), 40.3 (CH), 41.7 (CH), 49.4 (CH), 50.1 (C-13), 53.9 (NCH₂), 61.2 (d, $J=5.4$ Hz, OCH₂CH₃), 61.4 (d, $J=5.4$ Hz, OCH₂CH₃), 63.6 (OCH₂), 110.8 (d, $J=9.9$ Hz, C-2), 114.9 (d, $J=182.5$ Hz, C-4), 122.7 (C=CH), 126.0 (2C, C-3', and C-5'), 127.9 (2C, C-2', and C-6'), 131.4 (d, $J=1.8$ Hz, C-1), 131.5 (C-1'), 134.4 (d, $J=14.4$ Hz, C-10), 144.7 and 144.8 (C=CH and C-5), 151.9 (C-4'), 158.9 (C-3), 221.6 (C-17). ³¹P NMR δ (ppm): 18.2. MS m/z (%): 634 (100, [M + H]⁺).

4.2. Determination of antiproliferative activities

The antiproliferative properties of the newly synthesised triazoles (**11a,b**–**15a,b**) were determined on a panel of human adherent cancer cell lines of gynaecological origin. MCF-7 and MDA-MB-231

were isolated from breast cancers differing in biochemical background, while A2780 cells were isolated from ovarian cancer. The cancer selectivity of compound **12a** was tested on the non-cancerous mouse embryo fibroblast cell line NIH/3T3. All cell lines were purchased from European Collection of Cell Cultures (ECCAC, Salisbury, UK). Cells were cultivated in minimal essential medium supplemented with 10% foetal bovine serum, 1% non-essential amino acids and an antibiotic–antimycotic mixture. All media and supplements were obtained from Lonza Group Ltd., Basel, Switzerland. Near-confluent cancer cells were seeded onto a 96-well microplate (5000 cells/well) and, after overnight standing, 200 μ L new medium, containing the tested compounds at 10 and 30 μ M, was added. After incubation for 72 h at 37 °C in humidified air containing 5% CO₂, the living cells were assayed by the addition of 20 μ L of 5 mg/ml 3-(4,5-dimethylthiazol-2-yl)-2,5-diphenyl-tetrazolium bromide (MTT) solution. MTT was converted by intact mitochondrial reductase and precipitated as purple crystals during a 4-h contact period. The medium was next removed and the precipitated formazan crystals were dissolved in 100 μ L of DMSO during a 60-min period of shaking at 37 °C.

Finally, the reduced MTT was assayed at 545 nm, using a microplate reader utilising wells with untreated cells serving as control²⁷. In the case of the most active compounds (i.e. higher than 50% growth inhibition at 30 μ M), the assays were repeated with a set of dilutions, sigmoidal dose–response curves were fitted to the determined data and the IC₅₀ values (the concentration at which the extent of cell proliferation was half that of the untreated control) were calculated by means of GraphPad Prism 4.0 (GraphPad Software, San Diego, CA). All *in vitro* experiments were carried out on two microplates with at least five parallel wells. Stock solutions of the tested substances (10 mM) were prepared in DMSO. The highest DMSO content of the medium (0.3%) did not have any substantial effect on cell proliferation. Cisplatin (Ebewe Pharma GmbH, Unterach, Austria) was used as positive control.

4.3. Tubulin polymerisation assay

The effect of brominated triazole (**12a**) on tubulin polymerisation was tested with the HTS-Tubulin Polymerisation Assay Biochem Kit (Bio-Kasztel Ltd., Budapest, Hungary) according to the manufacturer's recommendations. Briefly, 10 μ L of a 0.125 or 0.25 mM solution of the test compound (**12a**) was placed on a prewarmed (37 °C), UV-transparent microplate. About 10 μ L 10 μ M paclitaxel and 10 μ L General Tubulin Buffer were used as positive and negative control, respectively. 100 μ L 3.0 mg/ml tubulin in 80 mM PIPES pH 6.9, 2 mM MgCl₂, 0.5 mM EGTA, 1 mM GTP was added to each sample, and the microplate was immediately placed into a prewarmed (37 °C) UV-spectrophotometer (SpectoStarNano, BMG Labtech, Ortenberg, Germany) to start the recording reaction. A 60-min kinetic measurement protocol was applied to determine the absorbance of the reaction solution per minute at 340 nm. For the evaluation of the experimental data, the maximum reaction rate (V_{\max} : Δ absorbance/min) was calculated. Moving averages of absorbances determined at three consecutive timepoints were calculated and the highest difference between two succeeding moving averages was taken as the V_{\max} of the tested compound in the tubulin polymerisation reaction. Each sample was prepared in two parallels and the measurements were repeated twice. For statistical evaluation, V_{\max} data were analysed by the one-way ANOVA test with the Newmann–Keuls post-test by using Prism 4.01 software (GraphPad Software, San Diego, CA).

4.4. Computational simulations

4.4.1. Docking studies

In all cases, the Glide package^{28,29} of the Schrodinger suit³⁰ was applied for docking calculations. Dimer structure with a colchicine analogue was cut out from crystal structure (pdb id: 3HKC, www.rcsb.org³¹) for colchicine binding side studies, and a monomer unit in complex with taxol was taken from taxol-stabilized microtubule (pdb id: 5SYF).

The protein preparation wizard³² was applied in the Maestro GUI³³ for the preparation of the downloaded rough crystal structures, and docking grids were prepared first. Each grid was centred to the original crystal ligand position, and default box size was applied. Following the grid generation, single precision (SP) docking was performed with enhanced ligand sampling. In the output, five poses were written out for each ligand.

4.4.2. Molecular dynamics calculations

The MD calculations were carried out with the Desmond^{34,35} program of the Schrodinger suit. OPLS3e forcefield³⁶ in combination with SPC explicit water model was applied in physiological salt concentration. Orthorhombic box with 10 Å buffer size was set up, and single strand 250 ns long NPT MD running was performed at 310 K after the relaxation of the system. The Nose–Hoover³⁷ thermostat and Martyna–Tobias–Klein barostat were applied with default relaxation times. The MMGBSA interaction energies were determined by taking 250 snapshots periodically from the MD trajectories and the thermal_mmgbsa.py script of the Desmond program was applied to calculate the binding free energy of a ligand.

5. Conclusions

In conclusion, new ring A modified 13 α -oestrone derivatives have been synthesised via directed combination of different structural elements. Certain new compounds displayed potent antiproliferative action against human reproductive cancer cell lines. 4-Bromo derivative **12a** exerted submicromolar cell growth-inhibitory action against A2780 cell line. Computational simulations reveal strong interactions of compound **12a** with colchicine and taxoid binding sites of tubulin. Direct effect of compound **12a** on microtubule formation was demonstrated via tubulin polymerisation assay.

Disclosure statement

No potential conflict of interest was reported by the author(s).

Funding

The work of Erzsébet Mernyák and Renáta Minorics in this project was supported by the János Bolyai Research Scholarship of the Hungarian Academy of Sciences. The work of Erzsébet Mernyák in this project was supported by the ÚNKP-19-4-SZTE-71, 'NEW NATIONAL EXCELLENCE PROGRAM OF THE MINISTRY OF HUMAN CAPACITIES. This work was supported by National Research, Development and Innovation Office-NKFIH through project OTKA SNN 124329. Support from Ministry of Human Capacities [Grant 20391–296 3/2018/FEKUSTRAT] is acknowledged.

References

- Gupta A, Kumar SB, Negi AS. Current status on development of steroids as anticancer agents. *J Steroid Biochem Mol Biol* 2013;137:242–70.
- Butenandt A, Wolff A, Karlson P. Über Lumi-oestron. *Chem Ber* 1941;74:1308–12.
- Yaremenko FG, Khvat AV. A new one-pot synthesis of 17-oxo-13 α -steroids of the androstane series from their 13 β -analogues. *Mendeleev Commun* 1994;187:187–8.
- Ayan D, Roy J, Maltais R, Poirier D. Impact of estradiol structural modifications (18-methyl and/or 17-hydroxy inversion of configuration) on the *in vitro* and *in vivo* estrogenic activity. *J Steroid Biochem Mol Biol* 2011;127:324–30.
- Schönecker B, Lange C, Kötteritzsch M, et al. Conformational design for 13 α -steroids. *J Org Chem* 2000;65:5487–97.
- Kaur R, Kaur G, Kaur Gill R, et al. Recent developments in tubulin polymerization inhibitors: an overview. *Eur J Med Chem* 2014;87:89–124.
- Steinmetz MO, Protá AE. Microtubule-targeting agents: strategies to hijack the cytoskeleton. *Trends Cell Biol* 2018;28:776–92.
- Naaz F, Haider MR, Shafi S, Yar MS. Anti-tubulin agents of natural origin: targeting taxol, vinca, and colchicine binding domains. *Eur J Med Chem* 2019;171:310–31.
- Cao YN, Zheng LL, Wang D, et al. Recent advances in microtubule-stabilizing agents. *Eur J Med Chem* 2018;143:806–28.
- Field JJ, Díaz JF, Miller JH. The binding sites of microtubule-stabilizing agents. *Chem Biol* 2013;20:301–15.
- Li W, Sun H, Xu S, et al. Tubulin inhibitors targeting the colchicine binding site: a perspective of privileged structures. *Future Med Chem* 2017;9:1765–94.
- Beale TM, Allwood DM, Bender A, et al. A-ring dihalogenation increases the cellular activity of combretastatin templated tetrazoles. *ACS Med Chem Lett* 2012;3:177–81.
- Liang L, Astruc D. The copper(I)-catalyzed alkyne-azide cycloaddition (CuAAC) “click” reaction and its applications. An overview. *Coord Chem Rev* 2011;255:2933–45.
- Szabó J, Jerkovic N, Schneider G, et al. Synthesis and *in vitro* antiproliferative evaluation of C-13 epimers of triazolyl-d-secoestrone alcohols: the first potent 13 α -d-secoestrone derivative. *Molecules* 2016;21:611–24.
- Bózsity N, Minorics R, Szabó J, et al. Mechanism of antiproliferative action of a new d-secoestrone-triazole derivative in cervical cancer cells and its effect on cancer cell motility. *J Steroid Biochem Mol Biol* 2017;165:247–57.
- Szabó J, Pataki Z, Wölfling J, et al. Synthesis and biological evaluation of 13 α -estrone derivatives as potential antiproliferative agents. *Steroids* 2016;113:14–21.
- Bacsa I, Herman BE, Jójárt R, et al. Synthesis and structure-activity relationships of 2- and/or 4-halogenated 13 β - and 13 α -estrone derivatives as enzyme inhibitors of estrogen biosynthesis. *J Enzyme Inhib Med Chem* 2018;33:1271–82.
- Jójárt R, Pécsy S, Keglevich G, et al. Pd-catalyzed microwave-assisted synthesis of phosphonated 13 α -estrones as potential OATP2B1, 17 β -HSD1 and/or STS inhibitors. *Beilstein J Org Chem* 2018;14:2838–45.
- Hirao T, Masunaga T, Ohshiro Y, Agawa T. Stereoselective synthesis of vinylphosphonate. *Tetrahedron Lett* 1980;21:3595–8.
- Keglevich G, Jablonkai E, László BB. A “green” variation of the Hirao reaction: the P-C coupling of diethyl phosphite, alkyl phenyl-H-phosphinates and secondary phosphine oxides with bromoarenes using a P-ligand-free Pd(OAc)₂ catalyst under micro-wave and solvent-free conditions. *RSC Adv* 2014;4:22808–16.
- Dziuganowska ZA, Ślepokura K, Volle JN, et al. Structural analogues of Selfotel (CGS-19755). *J Org Chem* 2016;81:4947–54.
- Keglevich G, Henyecz R, Mucsi Z, Kiss NZ. The palladium acetate-catalyzed microwave-assisted Hirao reaction without an added phosphorus ligand as a “green” protocol: a quantum chemical study on the mechanism. *Adv Synth Catal* 2017;359:4322–31.
- Matsumoto J, Ariyoshi N, Sakakibara M, et al. Organic anion transporting polypeptide 2B1 expression correlates with uptake of estrone-3-sulfate and cell proliferation in estrogen receptor-positive breast cancer cells. *Drug Metab Pharmacokin* 2015;30:133–41.
- Banerjee N, Allen C, Bendayan R. Differential role of organic anion-transporting polypeptides in estrone-3-sulphate uptake by breast epithelial cells and breast cancer cells. *J Pharmacol Exp Ther* 2012;342:510–09.
- Mernyák E, Szabó J, Bacsa I, et al. Syntheses and antiproliferative effects of D-homo- and D-secoestrones. *Steroids* 2014;87:128–36.
- Peyrat J-F, Brion J-D, Alami M. Synthetic 2-methoxyestradiol derivatives: structure-activity relationships. *Curr Med Chem* 2012;19:4142–56.
- Mosmann T. Rapid colorimetric assay for cellular growth and survival: application to proliferation and cytotoxicity assays. *J Immunol Methods* 1983;65:55–63.
- Friesner RA, Banks JL, Murphy RB, et al. Glide: a new approach for rapid, accurate docking and scoring. 1. Method and assessment of docking accuracy. *J Med Chem* 2004;47:1739–49.
- Halgren TA, Murphy RB, Friesner RA, et al. Glide: a new approach for rapid, accurate docking and scoring. 2. Enrichment factors in database screening. *J Med Chem* 2004;47:1750–9.
- Schrödinger Release 2019-4: Schrödinger, LLC, New York, NY, 2019.
- Berman HM, Westbrook J, Feng Z, et al. The protein data bank. *Protein Data Bank Nucleic Acids Res* 2000;28:235–42.
- Sastry GM, Adzhigirey M, Day T, et al. Protein and ligand preparation: parameters, protocols, and influence on virtual screening enrichments. *J Comput Aid Mol Des* 2013;27:221–34.
- Schrödinger Release 2019-4: Maestro, Schrödinger, LLC, New York, NY; 2019.
- Bowers KJ, Chow E, Xu H, et al. Scalable Algorithms for Molecular Dynamics Simulations on Commodity Clusters. *Proceedings of the ACM/IEEE Conference on Supercomputing (SC06)*, Tampa, FL, 2006, November 11–17.
- Schrödinger Release 2019-4: Desmond Molecular Dynamics System, D. E. Shaw Research, New York, NY, 2019.
- Harder E, Damm W, Maple J, et al. OPLS3: a force field providing broad coverage of drug-like small molecules and proteins. *J Chem Theory Comput* 2016;12:281–96.
- Hoover WG. Canonical dynamics: equilibrium phase-space distributions. *Phys Rev A* 1985;31:1695–7.